

7-29-2015

Impact and recovery of pH in marine sediments subject to a temporary carbon dioxide leak

Peter Taylor
Scottish Association for Marine Science

Anna Lichtschlag
National Oceanography Centre Southampton

Matthew Toberman
Scottish Association for Marine Science

Martin D.J. Sayer
Scottish Association for Marine Science

Andy Reynolds
Scottish Association for Marine Science

See next page for additional authors

Follow this and additional works at: <https://zuscholars.zu.ac.ae/works>



Part of the [Life Sciences Commons](#)

Recommended Citation

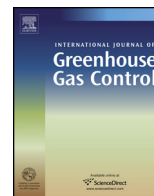
Taylor, Peter; Lichtschlag, Anna; Toberman, Matthew; Sayer, Martin D.J.; Reynolds, Andy; Sato, Toru; and Stahl, Henrik, "Impact and recovery of pH in marine sediments subject to a temporary carbon dioxide leak" (2015). *All Works*. 1938.

<https://zuscholars.zu.ac.ae/works/1938>

This Article is brought to you for free and open access by ZU Scholars. It has been accepted for inclusion in All Works by an authorized administrator of ZU Scholars. For more information, please contact Yrjo.Lappalainen@zu.ac.ae, nikesh.narayanan@zu.ac.ae.

Author First name, Last name, Institution

Peter Taylor, Anna Lichtschlag, Matthew Toberman, Martin D.J. Sayer, Andy Reynolds, Toru Sato, and Henrik Stahl



Impact and recovery of pH in marine sediments subject to a temporary carbon dioxide leak



Peter Taylor^{a,*}, Anna Lichtschlag^b, Matthew Toberman^a, Martin D.J. Sayer^{a,c}, Andy Reynolds^a, Toru Sato^d, Henrik Stahl^{a,e}

^a Scottish Association for Marine Science, Scottish Marine Institute, Oban PA37 1QA, Scotland

^b National Oceanography Centre, University of Southampton Waterfront Campus, European Way, Southampton, SO14 3ZH, England

^c NERC National Facility for Scientific Diving, Scottish Association for Marine Science, Oban PA37 1QA, Argyll, UK

^d Department of Ocean Technology, Policy and Environment, University of Tokyo, 5-1-5, Kashiwanoha, Kashiwa-shi, Chiba 277-8561, Japan

^e Zayed University, PO Box 19282, Dubai, United Arab Emirates

ARTICLE INFO

Article history:

Available online 1 October 2014

Keywords:

Carbon capture and storage

Sediment pore water

pH

CO₂

ABSTRACT

A possible effect of a carbon dioxide leak from an industrial sub-sea floor storage facility, utilised for Carbon Capture and Storage, is that escaping carbon dioxide gas will dissolve in sediment pore waters and reduce their pH. To quantify the scale and duration of such an impact, a novel, field scale experiment was conducted, whereby carbon dioxide gas was injected into unconsolidated sub-sea floor sediments for a sustained period of 37 days. During this time pore water pH in shallow sediment (5 mm depth) above the leak dropped >0.8 unit, relative to a reference zone that was unaffected by the carbon dioxide. After the gas release was stopped, the pore water pH returned to normal background values within a three-week recovery period. Further, the total mass of carbon dioxide dissolved within the sediment pore fluids above the release zone was modelled by the difference in DIC between the reference and release zones. Results showed that between 14 and 63% of the carbon dioxide released during the experiment could remain in the dissolved phase within the sediment pore water.

© 2014 The Authors. Published by Elsevier Ltd. This is an open access article under the CC BY license (<http://creativecommons.org/licenses/by/4.0/>).

1. Introduction

Increases in global atmospheric carbon dioxide levels leads to climate change and ocean acidification (Cao and Caldeira, 2008; Doney et al., 2009). Despite global efforts to increase energy efficiency and reduce demand on combustion of fossil fuels, atmospheric concentrations of carbon dioxide continue to rise (The Global CCS Institute, 2014). Different technologies are proposed to mitigate the impact of increasing atmospheric carbon dioxide concentrations. Carbon capture and storage (CCS) collects carbon dioxide from large point source emitters, such as a power stations or large industrial facilities. It is then compressed and transported to a suitable geological location for injection into a porous rock formation, overlain by a sealing cap rock, where it will be stored over geological timescales (IPCC, 2005).

As of yet, there is a lack of research on the environmental consequences that may arise from a leak of carbon dioxide from a sub-sea floor storage facility, particularly research that includes the

complexities of the natural environment (Blackford et al., in press). Several studies have attempted to fill this gap in knowledge by researching natural carbon dioxide seeps (Caramanna et al., 2011; Espa et al., 2010; Hall-Spencer et al., 2008; Vizzini et al., 2010). However, with this approach it is impossible to assess the rate with which “normal” conditions change following the start of the release and the rate with which they are re-established following termination of the release. Furthermore the hydrothermal nature of these systems leads to high background temperatures and contamination with traces of hydrogen, hydrogen sulphide and methane among other impurities, changing redox conditions and chemical reactions within the sediment (Italiano and Nuccio, 1991). Therefore, to test the impact and the rapidity of recovery after a CO₂ leak in the environment, a purposefully designed carbon dioxide release facility is needed.

In order to address this, a large-scale multi-disciplinary experiment was conducted in situ in a Scottish Sea Loch during the summer of 2012, to study the impacts of a simulated sub-sea floor leak of carbon dioxide on the marine environment. Carbon dioxide gas was released into unconsolidated sediment for a sustained period of 37 days (QICS, 2014; Taylor et al., 2015). During the QICS experiment a total of 4200 kg of carbon dioxide gas was

* Corresponding author. Tel.: +44 0 1631559000; fax: +44 0 1631559001.
E-mail address: pete.taylor@sams.ac.uk (P. Taylor).

injected into 11 m of unconsolidated sediment, in a water depth of 10–12 m. This resulted in migration of dissolved and gaseous carbon dioxide through the sediment overburden and gas bubbling from seabed pockmarks into the overlying water column (Lichtschlag et al., 2015). The QICS study area in Ardmucknish Bay (Blackford et al., in press; Taylor et al., 2015) has low water residence time, flushing being aided by the flow from nearby Loch Etive (Thorpe et al., 1983; Thorpe and Hall, 1983). It could, therefore, be anticipated that carbon dioxide enriched sea water from the release zone would be flushed from the bay within a few tidal cycles (Atamanchuk et al., 2015) and replaced with non-affected water from elsewhere.

However, the impact of the carbon dioxide on the sediments may not be straightforward. The dispersion of carbon dioxide saturated pore water from deeper down in the sediment overburden might be complex, as it can occur due to chemical diffusion along concentration gradients, vertical and horizontal displacements due to the difference in density between pore waters saturated with carbon dioxide and native fluids, and through the mechanical disturbance of bubble movement on unconsolidated sediments. The recovery of the sediment after an injection of carbon dioxide gas can be affected by several processes, including mineral buffering, sinking of carbon dioxide enriched pore water due to density differences and the replacement of non-affected sea water close to the sediment water interface through bioirrigation and/or pore water advection.

As carbon dioxide dissolves in water, it causes a shift in the natural carbonate system, causing the pH of sea water to drop and changing the saturation state of calcium carbonate (Zeebe and Wolf-Gladrow, 2001). Changes in the pH of pore water of sediments may have important consequences for fauna living therein (Murray et al., 2013) from loss of calcifying organisms (Hendriks et al., 2010) through to reductions in growth and survival rates (Fabry et al., 2008; Kroeker et al., 2010; Murray et al., 2013). Species may not all be impacted equally, resulting in the shifts in community structure and biodiversity, whether caused by susceptibility to alterations in pH or through excess carbon dioxide (Widdicombe and Spicer, 2008).

Marine sediments are essential for biogeochemical processes such as nutrient recycling, carbon remineralisation and carbon burial (Cai and Reimers, 2000; Cai et al., 2000; Canfield et al., 1993), which may be impacted by changes in benthic community structures caused by pH changes. Therefore, it is important to quantify the potential for large scale shifts in pH associated with a carbon dioxide leak, and the rate at which pH returns to background levels after the cessation of such a leak. Similarly, diffusion mediated oxygen flux in the sediment is a proxy for the rate at which microbes remineralise carbon (Glud, 2008) within the benthic sediments.

In addition to this, metals can be mobilised from marine sediments, that act as reservoirs for metals in various forms, e.g. as precipitates or as components of organic molecule complexes and detritus, being deposited on the seabed, hence removing the metals from the overlying water (Stumm and Morgan, 1996). It has been shown that these complexes are susceptible to changes in sediment pH (Payan et al., 2012), changes in the ambient carbonate system to which they are exposed and changes in oxygen concentrations (Ardelan et al., 2009; Little and Jackson, 2010; Stahl et al., 2012; Tankere-Muller et al., 2007).

The present study investigates the pH and oxygen dynamics of interstitial pore water within coastal surface sediments impacted by a release of carbon dioxide gas from a simulated carbon dioxide storage facility. It also examines how rapidly the sediment pore water returns to background values after the cessation of the leak and quantifies the amount of dissolved carbon dioxide required to match the observed changes in dissolved inorganic carbon within the sediment pore waters.

2. Materials and methods

2.1. Experiment site and description

The large-scale in situ carbon dioxide release experiment site was located in Ardmucknish Bay on the west coast of Scotland, with the release epicentre located 350 m off shore at 11 m depth below the sediment–water interface and with 10–12 m of overlying water column, depending on tidal state (Taylor et al., 2015). The carbon dioxide injection rate was increased by increments during the experiment, to maximise injection rate without fracturing the unconsolidated sediment (Taylor et al., 2015) around a 5 m long diffuser with an effective mesh size of 0.5 mm and an internal diameter of 2.8 cm. Sediment cores were collected for ex situ pH and oxygen microprofiling, using SCUBA diving, from two zones: (a) the release zone comprising the area within 10 m of the gas diffuser at the end of the release pipe, in the area with gas flow from the sediment and (b) a reference zone, 450 m away from the release point and unaffected by the CO₂ release (Taylor et al., 2015). Cores were collected from both of these locations on proximal dates so that a meaningful comparison could be generated at various time points. The experiment duration was counted in days, with day 0 being the initial day of carbon dioxide release into the sub sea floor sediments. The release phase lasted for a total of 37 days. After the release phase, there was an extended recovery monitoring programme. Core collection campaigns/times were chosen to best capture the impact and recovery process; at the end of the carbon dioxide release phase on days 35–36 (last week of release), on days 42–43 in the first week after the release was stopped and on days 57–61, 3 weeks after the release was stopped. Unfortunately, pH profiles were not generated prior to the release phase as planned, due to problems with experimental equipment.

2.2. pH profiling

Sediment cores with a 5 cm inner diameter and a total sediment core length of 10 to 15 cm, were collected from the release zone and reference zone, respectively. The cores were transported to a laboratory within 30 min of collection and placed in a temperature controlled aquarium, filled with bottom water from the same zone as the cores and maintained at in situ bottom water temperature (10–12 °C depending on the date). An immersion pump was placed in the aquarium, ensuring that the water was well stirred and homogenous and microprofiling was carried out in day-light conditions on each occasion. On each sampling occasion a minimum of three cores was collected from each zone.

LIX microelectrodes with a tip diameter of <10 μm, a soda glass shaft and a length of 40 cm were constructed as fully described in De beer et al. (1997) and in Queiros et al. (2015). Microelectrodes were calibrated using pre-made buffers with a pH of 4, 7 and 9 on the seawater scale. For calibration, electrodes were suspended in pH buffer solutions and the mV output was recorded prior to and after profiling in the sediment. Microprofiling was done manually, using a micromanipulator (Märzhäuser Weltzar GmbH, Type MM33 r.m. Kipp.) attached to a stand and positioned over the aquarium. The microelectrode was attached to a high impedance mV meter (JENCO Digital pH/mV meter 601A), with the reference electrode suspended in the aquarium water.

For profiling, the microelectrode was then placed into the water above the sediment and profiles with 100 μm increments were measured by recording the stable mV output after 10 s at each depth interval. Micro-profiles were recorded to a maximum depth of 1 cm, with the microprofile starting at least 1 mm above the sediment water interface. The latter was determined as the point at which the profile departed from a vertical pH profile, representing the uniformly mixed overlying water.

All microprofiles generated from a sampling location were then combined into an average profile for each sampling occasion. To remove erroneously high or low readings caused by the tip of the microelectrode colliding with obstacles in the sediment, a 3 point running average was applied. On each sampling occasion a minimum of three profiles was measured. Each core was profiled at least once, although typically cores were profiled twice, replicates from each core being limited due to breakage of the microelectrodes on shells and/or larger grains of sediment; profiles from the reference zone were collected and profiled within 4 days of those collected at the release zone so that seasonal changes and disturbances due to weather patterns could be discounted from any comparisons.

Profiles were analysed for any significant differences at a range of depth points: at 1 mm above the sediment–water interface, at the sediment–water interface and at 1, 2, 3, 4 and 5 mm below the sediment water–interface, using ANOVA.

2.3. Oxygen profiling

Oxygen concentration profiles were measured using the same micromanipulator as described above, with a Clark type microelectrode (Clark et al., 1953; Glud, 2008; Revsbech and Ward, 1983) attached to a pA meter (Unisense Picoammeter PA2000). The microelectrodes were made with a tip diameter of <15 μm . The profiles were measured simultaneously with the pH profiles and the steady state pA output from the microelectrode was also recorded after 10 s at each depth point. Typically the pH and oxygen microelectrodes were separated by less than 1 cm horizontally. The aquarium was open to free passage of air and the water was stirred by an immersion pump, so the water within the aquarium was assumed to be oxygen saturated. Zero % and 100% oxygen saturation was used to calibrate the pA output from the microelectrode. Oxygen concentration at saturation at the salinity and temperature determined in the aquarium on each sampling date was 271–284 $\mu\text{mol O}_2 \text{ L}^{-1}$. This was confirmed by determining the oxygen concentration in water samples after Winkler (1888) on two occasions. For the 0% oxygen calibration, a reading was taken from the bottom of the collected oxygen profiles, where the sediment was anoxic.

The depth of oxygen penetration was taken as the point at which the measured oxygen concentration within the sediment dropped below 3 $\mu\text{mol L}^{-1}$. The diffusive oxygen uptake into the sediment was calculated using Fick's first law of diffusion by calculating the diffusion gradient across the diffusive boundary layer (Glud, 2008; Revsbech et al., 1998) and using an oxygen diffusion coefficient of $1.4214 \times 10^{-5} \text{ cm}^2 \text{ s}^{-1}$ (salinity of 36, temperature of 9 °C (Ramsing and Gundersen, undated)).

2.4. Sediment porosity

Before the start of the QICS experiment, 10–15 cm long sediment samples were collected using a Craib corer. Cores were sliced into 2 cm sections for porosity analysis. Sediment was weighed and placed in an oven at 95 °C for 24 h before weighing again. The difference in volume was assumed to be evaporated water from the sediment, and thus representing a measure of porosity.

Although attempts were made to take longer cores in a near-by location, this was unsuccessful due to large boulders in the sediment preventing easy coring. Additionally, after selecting a drilling site where the sediment was thought to have fewer boulders, long gravity cores were not taken as there was a risk that the holes created by coring could act as an easy conduit to the sediment surface along which gas would preferentially migrate. Further estimates of sediment porosity in the deeper lithologies reported at the site

were gathered from literature sources identified in the results, Section 2.4.

3. Results

3.1. pH profiles

Vertical profiles of pH in sediment and the overlying water columns are shown in Fig. 1. Those collected from the reference zone show a stable pH of 8.2 above the sediment–water interface, representing the well mixed water, in all but one time point, at day 61. The profile on day 61 shows a small increase (of 0.08 pH units) towards the sediment–water interface. This is likely to be due to photosynthetic activity (Stahl et al., 2006), probably of microphytobenthos, absorbing carbon dioxide from the overlying sea water and thus increasing pH. This was not seen at the release zone on any sampling occasion.

At both the release zone and the reference zone, the pH decreased below the sediment–water interface. At the reference zone the pH decreases steadily for the first 3 mm, from a pH of 8.2 in the overlying water to a minimum of 7.7 on day 43, at a depth of 2.7 mm below sediment–water interface (Fig. 1b). Below this depth, sediment pH is more or less stable, or slightly increasing, with increasing depth.

These profiles from the reference zone can be contrasted with the pH profiles measured at the release zone, which in general have a similar shape, with a stable pH profile in the well mixed overlying water, a reduction in pH in the top 3 mm of the sediment, then constant values below this depth, except for the profile collected on day 42, which starts to become more alkaline with increasing depth below 3 mm (Fig. 1e). However, for profiles taken at the release zone absolute pH values are substantially lower, both in the water column and the sediments compared to profiles from the reference zone. As shown in Fig. 1, the pH not only starts at a noticeably lower value in the overlying sea water (Fig. 1e and f), but also continues to drop with increasing depth within the sediment to a minimum at 3 mm. The minimum pH attained at the release zone was 7.01 at 2.6 mm depth on day 42.

Statistical analysis, using ANOVA, showed that the pH profiles from the reference zone were not significantly different from each other at any depth or time point ($p=0.08$ to 0.56 depending on the depth point). At the release zone, the profiles taken on day 35 and 42 were significantly different from those collected on days 36 and 43 at the reference zone, respectively ($p < 0.03$). Additionally the two profiles from the release zone collected on days 35 and 42 were significantly different from each other ($p < 0.04$) at the sediment–water interface and above, but were not significantly different from each other below this point ($p = 0.06$ to 0.54 depending on depth point). The profiles taken from the release zone at day 57 were significantly different from the profiles taken in the release zone on day 35 and day 42 above 4 mm depth in the sediment, but were not significantly different from the reference zone pH profiles above 4 mm depth in the sediment at any time point.

3.2. Diffusive flux

Diffusive flux of oxygen into the sediment and oxygen penetration depth as determined with oxygen microelectrodes are shown in Figs. 2 and 3. In general, oxygen penetration was between 2 and 4 mm, both at the release and reference zones. Statistical analysis confirmed that the oxygen penetration depth is not significantly different between zones at proximal dates ($p=0.16$ on days 35–36 and 0.15 on days 42–43), except for the profiles taken on days 57–61, which are significantly different ($p=0.004$). On these occasions, the release zone had the deepest oxygen penetration depth.

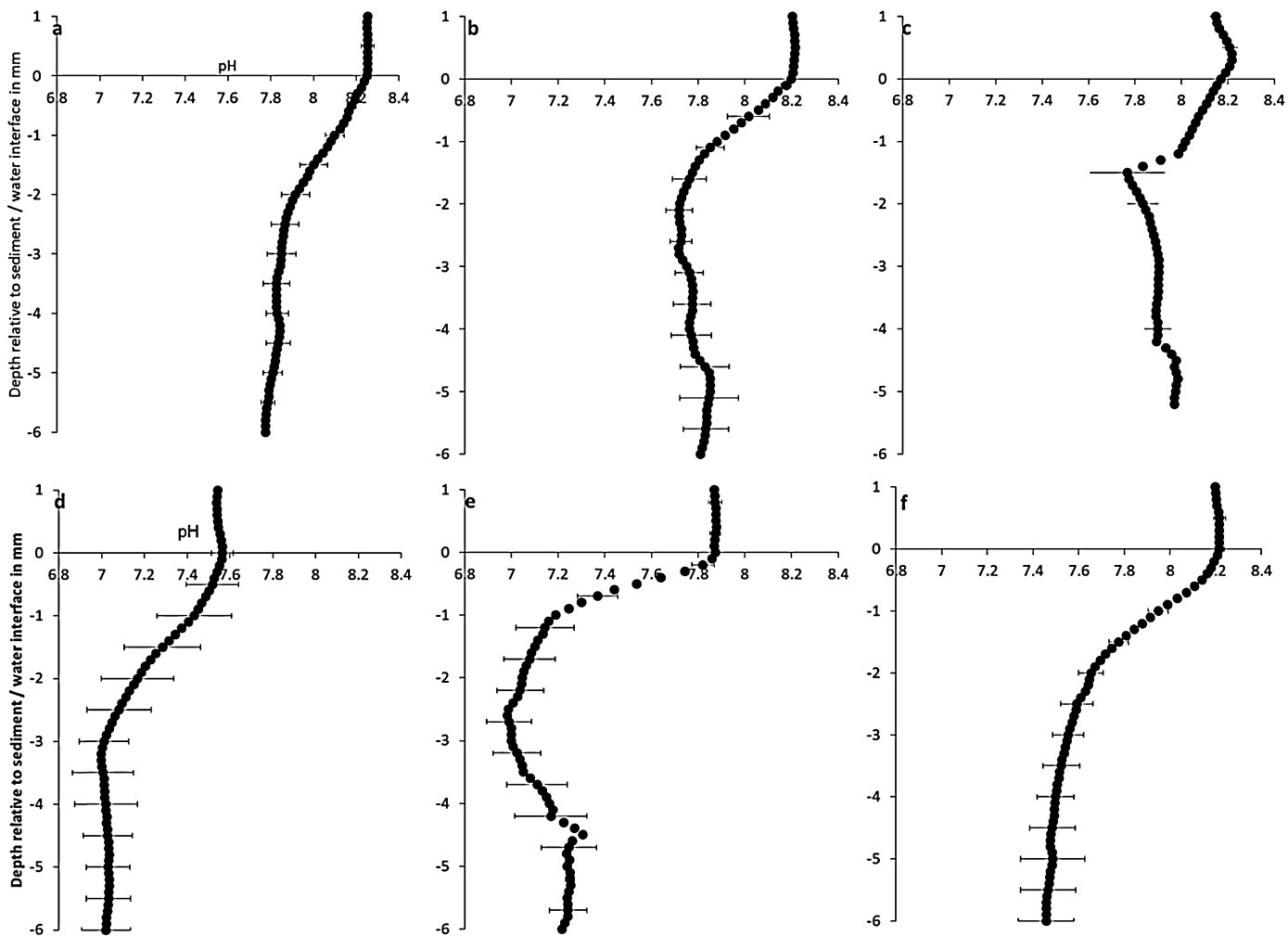


Fig. 1. pH microprofiles taken during the QICS experiment, from the reference zone: top row (a)–(c) and release zone: bottom row (d)–(f). Displayed profiles are a mean of 3 cores, with a 3 point running average and \pm st dev displayed at every 0.5 mm. (a) Represents the profiles collected at the reference zone on day 36, (b) = reference zone at day 43, (c) = reference zone at day 61, (d) = release zone at day 35, (e) = release zone at day 42, (f) = release zone at day 57 nb, on profile c, standard deviation bars are not visible at this scale in several cases.

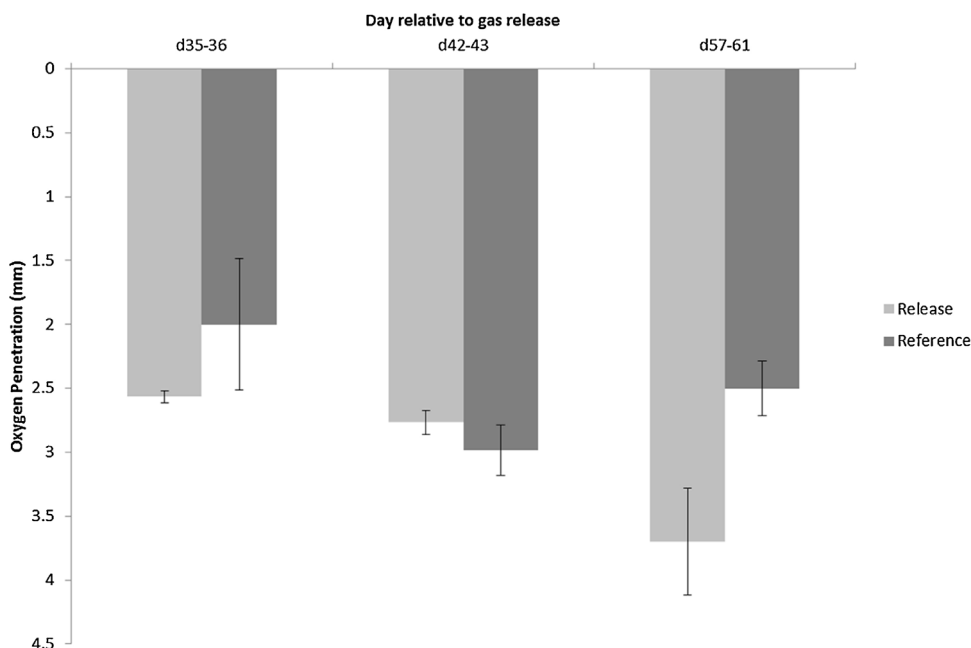


Fig. 2. Oxygen penetration depth of the release and reference zones on proximal dates, with error bars showing standard deviation.

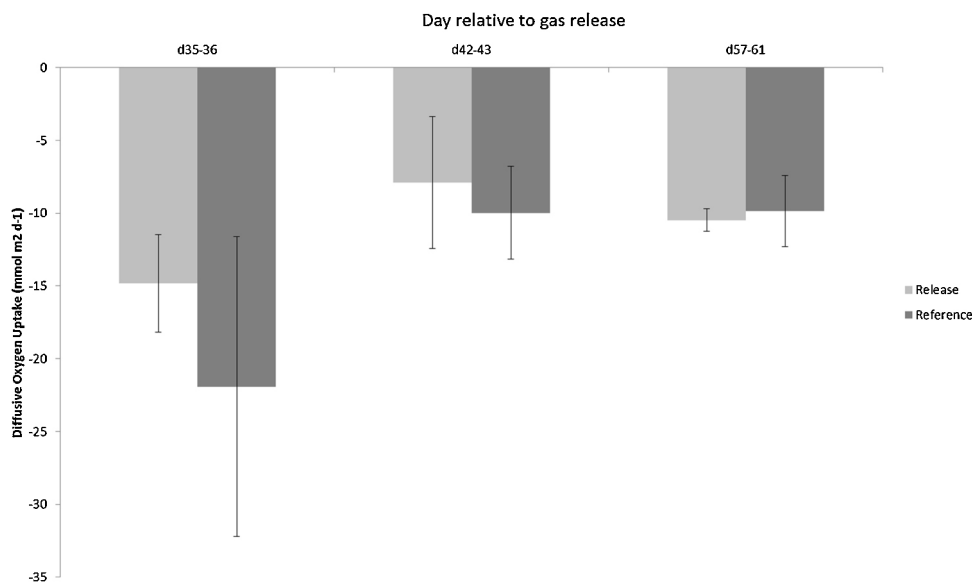


Fig. 3. Diffusion mediated oxygen flux into the sediment of the release and reference zones.

The diffusion mediated oxygen uptake was calculated from the oxygen profiles and is displayed in Fig. 3. ANOVA analysis shows that there are no significant differences between the two zones at proximal dates (p between 0.68 and 0.37). The values vary from $-7.9 \text{ mmol m}^{-2} \text{ d}^{-1}$ to $-21.9 \text{ mmol m}^{-2} \text{ d}^{-1}$ with maximal fluxes at each zone measured on days 35–36. However, there is no significant difference between the fluxes measured at these dates and the fluxes measured on days 42 and 43.

3.3. Sediment porosity

Three lithologies were identified from geophysical examination of the site, the top lithology of fine to coarse sand, the second lithology of very fine sand and below this a medium silt to mud. Of the three lithologies present in the sediment above the carbon dioxide release point, 11 m below the sediment–water interface, only the top one was measured directly. The mean porosity of this lithology was calculated as 0.49 over the core depths, (data range: 0.32–0.64; standard deviation = 0.09), which was applied to the top lithology (shelly coarse to fine sands up to 1.2 m below the sediment surface). The second lithology, down to 2.75 m is fine to very fine sands, with an assumed porosity of 0.55 (Rosas et al., 2014). The third lithology of very fine to medium silts/muds was assumed to have a porosity of 0.68, based on the fine grain size expected for this lithology (Lee et al., 2013). More detailed information on the lithologies present is discussed by (Taylor et al., 2015). Information in Lichtschlag et al. (2015) show that the total inorganic carbon (TIC) content of the sediment in the release zone was 0.08% dry weight at 0–2 cm below the sediment water interface. Furthermore, the DIC content of the sediment pore water was measured as $29,300 \mu\text{mol kg}^{-1}$ in the release zone as opposed to $2600 \mu\text{mol kg}^{-1}$ in the reference zone, measured at 30 cm below the sediment water interface (Blackford et al., in press).

4. Discussion

During the QICS experiment, a total of 4200 kg of carbon dioxide gas was released into the sediments, 11 m below the sediment water interface which was 12 m below the mean sea level (Blackford and Kita, 2013; Blackford et al., in press; Taylor et al., 2015). After 35 days of injection, pore water enriched in dissolved carbon dioxide had reached the upper 30 cm of the surface sedi-

ments and highest concentrations in the sediments were found at day 42, i.e. one week after the injection was stopped (Blackford et al., Lichtschlag et al.). The fact that the pH profiles measured in the reference zone, 450 m distant to the release zone, show no significant difference during or after the carbon dioxide release, and that pH values are typical for coastal waters (pH \sim 8.2 above sediment), indicates that the reference zone remained unaffected by the injected gas during the entire length of this experiment. This is also supported by Atamanchuck et al. (2014), reporting elevated $p\text{CO}_2$ concentrations in the bottom water in the close vicinity of the release epicentre, and no traces of the injected carbon dioxide away from the epicentre. Additionally, no indications of increased pore water DIC concentrations were present beyond the borders of the release zone (Lichtschlag et al., 2015).

The release zone had significantly reduced pH in sediment pore waters as well as in the overlying sea water compared to the reference zone (Fig. 1). 48 h prior to termination of the carbon dioxide release (day 35), a reduction of 0.84 pH units was measured between 2 and 3 mm depth in the sediment of the release zone, whereas the pH was xx in the reference zone (Fig. 1d). This confirms that the pH changes observed at the release zone are associated with the injected gas, rather than with disturbances caused by changes in the circulation patterns in near-by Loch Etive, as described in (Overnell et al., 2002) or by local weather driven events such as sediment re-suspension caused e.g. by a passing storm as such large-scale changes would impact both the release and reference zone equally. Weather data for the period of the experiment, obtained from a local weather station shows that no such event took place (Scottish Association for Marine Science, 2013). It has also been shown that, for marine sediments of the same type, millimetre scale variation is often as significant as variation over larger scales (Glud et al., 2009), suggesting that such a profound change in pH of sediment pore water is solely due to the carbon dioxide release, as the observed reduction is consistent over both the sub cm scale within cores as well as the larger, between core scale. (Lichtschlag et al., 2015) could determine the origin of the carbon dioxide through its isotopic composition, which further confirms that the pH changes observed at the release zone is associated with the injected carbon dioxide.

At the reference zone on day 61 (Fig. 1c) the profile is of unusual shape. This is partly due to photosynthesis at the sediment surface, reducing the pH of the sea water immediately overlying the

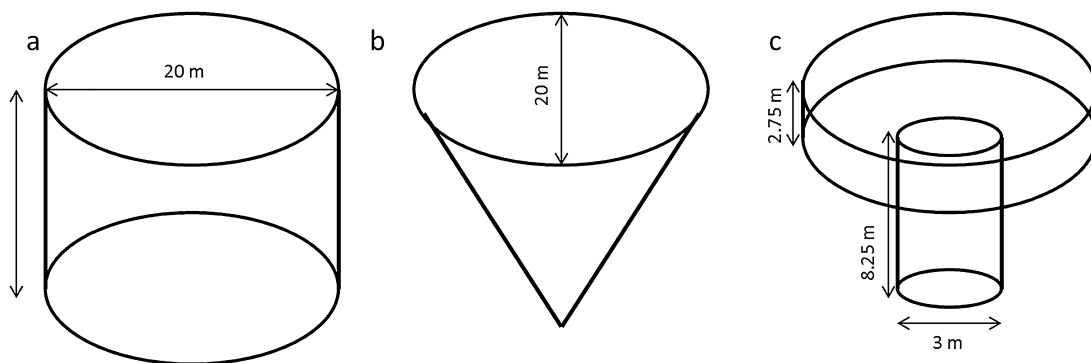


Fig. 4. Three shapes of possible CO₂ plumes within the sediment, from which pore water volumes were calculated.

sediment in one of the profiles, but is also due to one of the profiles taken hitting a large grain of material at 1.5 mm depth, causing a sharp decrease in recorded pH. Unfortunately, on this sampling occasion it was only possible to do three microprofiles, one from each core collected, before the microelectrode broke, limiting the data set.

Hence, it is clear from these data that the injected gas dissolved in the pore water, had an effect on the pH of sediment pore waters within the release zone and that this significant and sustained reduction in the pore water pH was separated from the reference zone 450 m away. The profiles collected at the reference zone are similar to pH profiles gathered from other locations (Marton and Roberts, 2014; Stahl et al., 2006), with those collected from the release zone similar to more extreme environments where the pH is naturally reduced due to geochemical reactions in the sediment, e.g. mud volcanoes (Lichtschlag et al., 2010; Preisler et al., 2007). The pH profiles that were collected in the release zone show a similar shape as the profiles from the reference zone, but with obvious changes to absolute pH throughout the profile, which is particularly evident towards the end of the carbon dioxide release phase on days 35 and 36. As highlighted in the results section above, the pH profile on day 42 from the release zone (Fig. 1e) shows an increasing pH with depth below a point of 3 mm. This could be explained by buffering of pH changes in the sediment by carbonate dissolution, that would lead to an increase of pH as described by (Blackford et al., in press).

It has been shown that during the QICS experiment, carbon dioxide gas was observed bubbling out of the sediment within hours of the initiation of gas release and that, similarly, it stopped bubbling out of the sediment within hours of the cessation of the gas release phase (Blackford et al., in press). The pH profiles show that the lowest pH was recorded at the end of the gas release phase of the experiment, on day 35, whereas Lichtschlag et al. (2015) report that the highest occurrence of DIC within the sediment was on day 42, after the carbon dioxide release phase. This indicates that the sediment may have been buffering pH changes within the pore water through carbonate dissolution.

Within only 3 weeks of stopping carbon dioxide release into the sediment, the pH of the sediment pore waters within 4 mm of the sediment water interface had largely recovered. It is possible that pH of the pore waters at the release zone started to recover to values more similar to the reference zone from the sediment–water interface with turbulent movement of sea water causing pore water replacement close to the sediment surface as evidenced by the statistical difference in pH at and above the sediment–water interface at the release zone.

The diffusive oxygen flux can be used as a proxy for organic carbon mineralisation as mediated by microbes and some meiofauna (Glud, 2008). The diffusion mediated oxygen uptake, with values of about $-7.9 \text{ mmol m}^{-2} \text{ d}^{-1}$ to $-21.9 \text{ mmol m}^{-2} \text{ d}^{-1}$ at both the release

zone and the reference zone, are similar to results from other coastal sediments (Wang et al., 2013). This ties in with the fact that microbes are routinely exposed to an environment with a highly variable pH, which can alter by as much as 0.4 or 0.5 pH units in 24 h (Stahl et al., 2006). The lack of significant differences between the two zones at the different time points agrees with simultaneously measured DIC flux data, showing values between 14 and $32 \text{ mmol m}^{-2} \text{ d}^{-1}$ (published as supplement to Blackford et al., in press), which is an important confirmation to the oxygen dynamics reported here. The vast majority of oxygen that enters the sediment is converted to carbon dioxide as the dominant respiration product, which is then exchanged across the sediment water interface as dissolved inorganic carbon (Glud, 2008). Therefore, if there is no significant difference in DIC flux recorded during the experiment it is unlikely that there would be a significant difference in diffusive oxygen uptake into the sediment either.

That said, there was a significant difference in the oxygen penetration depth in the release zone 21 days after the release had stopped, when comparing days 57 and 61, although there were no significant differences on other dates. Taken alone, this suggests a reduced consumption of oxygen within the sediment, however, the diffusion mediated oxygen consumption indicates otherwise, although this result is probably a sampling artefact. It is possible that this represents a reduction of microbial activity close to the sediment surface allowing increased activity at deeper levels as the sediment becomes re-oxygenated, with effects of the released carbon dioxide already observed on microbes by day 14 (Tait et al., 2015).

The removal of the sediment cores, their transfer and immediate immersion in an aquarium will cause changes in pH and oxygen profiles in the sediment, when measured in the laboratory. During the QICS experiment there was a release of carbon dioxide within the sediment, with the observation of bubbles leaving the sediment, rendering it impossible to fully replicate the in situ conditions in the laboratory (Blackford et al., in press). However, cores were always transferred to a temperature controlled aquarium and their analysis commenced within 30 min of the core being taken from the sediment to minimise the risk of potential sampling artefacts. Furthermore, cores were always immersed in bottom water, collected from the same zone as the cores and they were maintained within the observed temperature range in the bay that day, with stirring to simulate the natural water movement in the bay. The possibility of obtaining the profiles in situ, using benthic lander technology was examined prior to the start of the experiment. However, benthic landers have a large foot-print (in the order of 1.5 m by 1.5 m) and due to the concentration of monitoring equipment in the different zones investigated during the QICS experiment, this option had to be discarded due to the risk of accidentally lowering the lander onto equipment previously deployed, damaging both this equipment and the lander.

Table 1

Volume of 3 modelled shapes depicting possible influence for CO₂ during migration through the sediment. The volume of pore water in the modelled shape is calculated by using a mean porosity of 0.49 for the top 1.2 m of sediment, a value of 0.55 for the next 1.55 m of sediment and a value of 0.68 for the sediment between 2.75 m depth and the release point at 11 m depth in the sediment. Density of the sea water is calculated using 11 decibar pressure, at 10° C and a salinity of 24, with the UNESCO equation of state, giving 1026 kg m⁻³. Excess carbon dioxide is calculated by the difference between the combined total of the calculated HCO₃⁻, CO₃ and CO₂ between the release and reference zone in Table 2 Radius (*r*) of 10 m, height (*h*) of 11 m, unless otherwise stated.

Model shape	Calculation	Volume (m ³)	Pore water (m ³)	Mass of water (kg × 10 ⁴)	Excess CO ₂ in model (mol)	Excess CO ₂ in pore water (kg)
Cylinder (Fig. 4a)	$V = \pi \times r^2 \times h$	3454	2215	227.2	60,666	2765
1 Cone (Fig. 4b)	$V = (\pi \times r^2 \times h) / 3$	1151	738	75.7	20,222	892
Funnel (Fig. 4c)	$V = (\pi \times 1.5)^2 \times 8.25 + (\pi \times r^2 \times 2.75)$	922	492	50.4	13,481	595

One question that has arisen during the QICS experiment is the final fate of the carbon dioxide gas released into the sediment. Although divers observed gas bubbling from the sediment into the overlying sea water (Blackford et al., *in press*), only about 15% of the total carbon dioxide was released as gas bubbles into the water column (Blackford et al., *in press*; Dewar et al., 2015). Away from the bubble streams the release of dissolved carbon dioxide from the sediment into the water column, as measured directly with benthic chambers, was not increased in the release zone compared to the reference zone, indicating that it is likely that no carbon dioxide left the sediment in dissolved form (Blackford et al., *in press*). This means that 85% of the injected carbon dioxide gas is currently unaccounted for in the sediments. Using the dissolved inorganic carbon content of the pore water (Blackford et al., *in press*; Lichtschlag et al., 2015), and making the assumptions that the increased DIC in the sediment pore water is uniformly spread in the release zone identified by geophysical investigation reported in Cevatoglu et al. (2015) and is the result of the carbon dioxide release it is possible to quantify the amount of carbon dioxide remaining in the sediment pore waters and not accounted for by either dissolved or gaseous flux from the sediment. It is apparent that the carbon dioxide injected may be present as one of several phases in the sediment, whether dissolved in the pore water, precipitated in the mineral phase or as bubbles of gas trapped within the sediment. This method of calculation will quantify the total amount of dissolved carbon dioxide present within the sediment pore water in between the diffuser and the sediment surface.

It has been shown that the carbon dioxide that was released into the sediment reached the sea floor in an area that could be loosely constrained by a circular area with a 20 m diameter (Cevatoglu et al., 2015). This area was calculated to be 314 m², with a sediment depth of 11 m from the carbon dioxide gas diffusion point. Taking these estimates, the volume of sediment can be calculated employing three simple possible patterns for gas migration through the sediments (Fig. 4). The three models were chosen to represent migration possibilities within the sediment on simplified scales. First, there was the possibility that the gas diffused from the release point horizontally before migrating upwards through the sediment (Fig. 4a). This is considered to be the least likely of the three scenarios as it only poorly matched observed seismic data (Cevatoglu et al., 2015). Second, is the possibility that the gas diffused horizontally at a constant rate while migrating upwards (Fig. 4b). This is thought to be more realistic than the first scenario, but takes no account of observed changes in geological structures within the sediment. Third, is the possibility that the gas migrated vertically up chimneys caused by micro-fracturing of the cohesive muddy sediment until it reached a permeable strata, at which point it rapidly diffused horizontally while migrating the last 2.75 m to the sediment surface (Fig. 4c); this is most closely supported by the observed geology and seismic data (Cevatoglu et al., 2015). Total volumes of sediment and pore waters in the different scenarios are given in Table 1.

The total volumes of the pore water for each of the models was then calculated by integrating the sediment depth horizons and the calculated or estimated porosities to the models, multiplying the sediment volume with the porosity value outlined in the materials and methods above, giving pore water volumes of between 2214 and 492 m³ (Table 1). Using the salinity (34), temperature (10° C) and 11 decibar pressure, the water can be converted to a mass using the UNESCO equation of state (Dalhousie, undated).

The additional carbon dioxide in the pore water is calculated by the difference in DIC between the reference and release zones, as reported in (Blackford et al., *in press*), with a value of 29,300 μmol kg⁻¹ in the release zone as opposed to 2600 μmol kg⁻¹ in the reference zone, measured at 30 cm below the sediment water interface. This is then converted to an absolute mass of carbon dioxide, calculated to remain within the sediment pore water for each of the three different models, with values ranging between 2675 and 594 kg of carbon dioxide dissolved, in various phases, within the sediment pore water. This represents between 63 and 14% of the carbon dioxide injected into the sediment during the QICS experiment, with the 14% figure being regarded as more likely given geophysical data available, due to the presence of narrow chimneys of microfractures up which the carbon dioxide gas bubbled (Cevatoglu et al., 2015). However uncertainty remains in as much as the chimneys are hypothesised to be mobile, with a network of microfractures activating and deactivating over time. Given a snap-shot image of the sediment, the lower estimate of mass of gas within the sediment is most plausible, but given the chimney mobility, the number could be much higher. Nevertheless, the numbers generated here agree with those calculated by (Mori et al., 2015), who used sophisticated modelling to estimate the amount of carbon dioxide remaining within the sediments as being between 10 and 40% of the injected gas.

Only a maximum of 15% (Dewar et al., 2015) (630 kg) of the gas released during the experiment was estimated to contribute to the observed bubble streams. Here a further 63–14% of the released carbon dioxide is accounted for as the mass required to increase the DIC in the surface sediments (Table 1) by the observed amount. It is apparent then that a large amount of the carbon dioxide released during the experiment is unaccounted for using the approach of the present study and the direct measurement of gas bubbles or the flux of DIC from the sediment into the overlying water (Blackford et al., *in press*; Dewar et al., 2015).

The pH of sediment pore waters within 4 mm of the sediment water interface was not significantly different from the reference zone within three weeks following the cessation of carbon dioxide release, although at this depth and below, significant differences remained. Further investigations are required to ascertain the cause of the return to normal pH levels. It could have been caused by chemical processes such as buffering caused by carbonate dissolution within the sediment, or by tidal flushing replacing the pore water close to the sediment–water interface.

The diffusion mediated oxygen uptake into the sediment indicates that there was little alteration to rates of microbial activity

during the release phase of the QICS experiment, when comparing the release and reference zones.

Acknowledgements

Funding for this experiment was provided by NERC (NE/H013962/1), the Scottish Government. We thank the Tralee Bay Holiday Park, Lochnell Estates and the inhabitants of Benderloch for hosting the experiment. We acknowledge Marine Scotland and The Crown Estate for permissions to carry out the work. The NERC National Facility for Scientific Diving, the crew of the R. V. Seol Mara based at SAMS provided operational support. Peter Taylor's Ph.D. studentship is funded by the European Social Fund. We thank the two anonymous reviewers for their input, which strengthened this manuscript.

References

- Ardelan, M.V., Steinnes, E., Lierhagen, S., Linde, S.O., 2009. Effects of experimental CO₂ leakage on solubility and transport of seven trace metals in seawater and sediment. *Sci. Total Environ.* 407, 6255–6266.
- Atamanchuk, D., Tengberg, A., Aleynik, D., Fietzek, P., Shitashima, K., Lichtschlag, A., Hall, P.O.J., Stahl, H., 2015. Detection of CO₂ leakage from a simulated sub-seabed storage site using three different types of pCO₂ sensors. *Int. J. Greenhouse Gas Control* 38, 121–134.
- Blackford, J., Stahl, H., Bull, J. M., Berges, B. J. P., Cevatoglu, M., Lichtschlag, A., Connelly, D., James, R. H., Kita, J., Long, D., Naylor, M., Shitashima, K., Smith, D., Taylor, P., Wright, I., Akhurst, M., Chen, B., Gernon, T. G., Houghton, C., Hayashi, M., Kaieda, H., Leighton, T. G., Sato, T., M.D.J., S., Suzamura, M., Tait, K., Vardy, M. E., P.R., W. & Widdicombe, S. Detection and impacts of leakage from sub-seafloor Carbon Dioxide Storage. *Nature Climate Change* doi 10.1038/nclimate2381.
- Blackford, J.C., Kita, J., 2013. A novel experimental release of CO₂ in the marine environment to aid monitoring and impact assessment. *Energy Procedia* 37, 3387–3393.
- Cai, W.-J., Zhao, P., Wang, Y., 2000. pH and pCO₂ microelectrode measurements and the diffusive behaviour of carbon dioxide species in coastal marine sediments. *Mar. Chem.* 70, 133–148.
- Cai, W.J., Reimers, C.E., 2000. Sensors for in situ pH and pCO₂ measurements in seawater and at the sediment–water interface. In: Buffle, J., Horvai, G. (Eds.), *In Situ Monitoring of Aquatic Systems: Chemical Analysis and Speciation*, pp. 75–119. ISBN 978-0-471-48979-5.
- Canfield, D.E., Jorgensen, B.B., Fossing, H., Glud, R., Gundersen, J., Ramsing, N.B., Thamdrup, B., Hansen, J.W., Nielsen, L.P., Hall, P.O.J., 1993. Pathways of organic carbon oxidation in three continental margin sediments. *Mar. Geol.* 113, 27–40.
- Cao, L., Caldeira, K., 2008. Atmospheric CO₂ stabilization and ocean acidification. *Geophys. Res. Lett.* 35 (19), 35.
- Caramanna, G., Voltattorni, N., Maroto-Valer, M.M., 2011. Is Panarea Island (Italy) a valid and cost-effective natural laboratory for the development of detection and monitoring techniques for submarine CO₂ seepage? *Greenhouse Gases: Sci. Technol.* 1, 200–210.
- Cevatoglu, M., Bull, J.M., Vardy, M.E., Gernon, T.G., Wright, I.C., Long, D., 2015. Gas migration pathways, controlling mechanisms and changes in sediment physical properties observed in a controlled sub-seabed CO₂ release experiment. *International Journal of Greenhouse Gas Control* 38, 26–43.
- Clark, L.C., Wolf, R., Granger, D., Taylor, Z., 1953. Continuous recording of blood oxygen tensions by polarography. *J. Appl. Physiol.* 6, 189–193.
- Dalhousie, P. O. A. undated. UNESCO Equation of State (density in terms of Salinity, Temperature and Pressure) [Online]. <http://www.phys.ocean.dal.ca/~kelley/seawater/density.html>. [Accessed 11/06/2014].
- De beer, D., Glud, A., Epping, E., Kuhl, M., 1997. A fast-responding CO₂ microelectrode for profiling sediments, microbial mats, and biofilms. *Limnol. Oceanogr.* 42, 1590–1600.
- Dewar, M., Sellami, N., Chen, B., 2015. Dynamics of rising CO₂ bubble plumes in the QICS field experiment: Part 2 - Modelling. *International Journal of Greenhouse Gas Control* 38, 44–51.
- Doney, S.C., Fabry, V.J., Feely, R.A., Kleypas, J.A., 2009. Ocean acidification: the other CO₂ problem. *Annu. Rev. Mar. Sci.* 1, 169–192.
- Espa, S., Caramanna, G., Bouché, V., 2010. Field study and laboratory experiments of bubble plumes in shallow seas as analogues of sub-seabed CO₂ leakages. *Appl. Geochem.* 25, 696–704.
- Fabry, V.J., Seibel, B.A., Feely, R.A., Orr, J.C., 2008. Impacts of ocean acidification on marine fauna and ecosystem processes. *ICES J. Mar. Sci.* 65, 414–432.
- Glud, R.N., 2008. Oxygen dynamics of marine sediments. *Mar. Biol. Res.* 4, 243–289.
- Glud, R.N., Stahl, H., Berg, P., Wenzhofer, F., Oguri, K., Kitazato, H., 2009. In situ microscale variation in distribution and consumption of O₂: a case study from a deep ocean margin sediment (Sagami Bay, Japan). *Limnol. Oceanogr.* 54, 1–12.
- Hall-Spencer, J.M., Rodolfo-Metalpa, R., Martin, S., Ransome, E., Fine, M., Turner, S.M., Rowley, S.J., Tedesco, D., Buia, M.-C., 2008. Volcanic carbon dioxide vents show ecosystem effects of ocean acidification. *Nature* 454, 96–99.
- Hendriks, I.E., Duarte, C.M., Álvarez, M., 2010. Vulnerability of marine biodiversity to ocean acidification: a meta-analysis. *Estuarine, Coastal Shelf Sci.* 86, 157–164.
- IPCC, 2005. Carbon Dioxide Capture and Storage. Cambridge University Press, The Edinburgh Building, Shaftesbury Road, Cambridge, 536 CB2 2RU, England.
- Italiano, F., Nuccio, P.M., 1991. Geochemical investigations of submarine volcanic exhalations to the east of Panarea, Aeolian Islands, Italy. *J. Volcanol. Geotherm. Res.* 46, 125–141.
- Kroeker, K.J., Kordas, R.L., Crim, R.N., Singh, G.G., 2010. Meta-analysis reveals negative yet variable effects of ocean acidification on marine organisms. *Ecol. Lett.* 13, 1419–1434.
- Lee, J.Y., Kim, G.Y., Kang, N.K., Yi, B.Y., Jung, J.W., Im, J.H., Son, B.K., Bahk, J.J., Chun, J.H., Ryu, B.J., Kim, D.S., 2013. Physical properties of sediments from the Ulleung Basin, East Sea: results from second Ulleung Basin gas hydrate drilling expedition, East Sea (Korea). *Mar. Pet. Geol.* 47, 43–55.
- Lichtschlag, A., Felden, J., Bruchert, V., Boetius, A., de Beer, Dirk, 2010. Geochemical processes and chemosynthetic primary production in different thiotrophic mats of the Hakon Mosby Mud Volcano (Barents Sea). *Limnol. Oceanogr.* 55, 931–949.
- Lichtschlag, A., James, R.H., Stahl, H., Connelly, D., 2015. Effect of a controlled sub-seabed release of CO₂ on the biogeochemistry of shallow marine sediments, their pore waters, and the overlying water column. *Int. J. Greenhouse Gas Control* 38, 80–92.
- Little, M.G., Jackson, R.B., 2010. Potential impacts of leakage from deep CO₂ geosequestration on overlying freshwater aquifers. *Environ. Sci. Technol.* 44, 9225–9232.
- Marion, J.M., Roberts, B.J., 2014. Spatial variability of phosphorus sorption dynamics in Louisiana salt marshes. *J. Geophys. Res.: Biogeosci.* 119, 2013JG002486.
- Mori, C., Sato, T., Kano, Y., Oyama, H., Aleynik, D., Tsumune, D., Maeda, Y., 2015. Numerical study of the fate of CO₂ purposefully injected into the sediment and seeping from seafloor in Ardmucknish Bay. *International Journal of Greenhouse Gas Control* 38, 153–161.
- Murray, F., Widdicombe, S., Mcneill, C.L., Solan, M., 2013. Consequences of a simulated rapid ocean acidification event for benthic ecosystem processes and functions. *Mar. Pollut. Bull.* 73, 435–442.
- Overnell, J., Brand, T., Bourgeois, W., Statham, P.J., 2002. Manganese dynamics in the water column of the upper basin of Loch Etive, a Scottish Fjord. *Estuarine, Coastal Shelf Sci.* 55, 481–492.
- Payan, M.C., Verbinnen, B., Galan, B., Coz, A., Vandecasteele, C., Viguri, J.R., 2012. Potential influence of CO₂ release from a carbon capture storage site on release of trace metals from marine sediment. *Environ. Pollut.* 162, 29–39.
- Preisler, A., de Beer, Dirk, Lichtschlag, A., Lavik, G., Boetius, A., Jorgensen, B.B., 2007. Biological and chemical sulfide oxidation in a Beggiatoa inhabited marine sediment. *Int. Soc. Microb. Ecol. J.* 1, 341–353.
- QICS, 2014. QICS Web Page [Online]. (<http://www.bgs.ac.uk/qics/:BGS>) [Accessed 21-01-2014 2014].
- Queiros, A.M., Taylor, P., Cowles, A., Reynolds, A., Stahl, H., Widdicombe, S., 2015. Optical assessment of impact and recovery of sedimentary pH profiles in ocean acidification and carbon capture and storage research. *International Journal of Greenhouse Gas Control* 38, 110–120.
- Ramsing, N. & Gundersen, J. undated. 2014 Seawater and Gases; Tabulated physical parameters of interest to people working with microsensors in marine systems, *Unisense*.
- Revsbech, N.P., Nielsen, L.P., Ramsing, N.B., 1998. A novel microsensor for determination of apparent diffusivity in sediments. *Limnol. Oceanogr.* 43, 986–992.
- Revsbech, N.P., Ward, D.M., 1983. Oxygen microelectrode that is insensitive to medium chemical composition: use in an acid microbial mat dominated by Cyanidium caldarium. *Appl. Environ. Microbiol.* 45, 755–759.
- Rosas, J., Lopez, O., Missimer, T.M., Coulibaly, K.M., Dehwah, A.H.A., Sesler, K., Lujan, L.R., Mantilla, D., 2014. Determination of hydraulic Conductivity from grain-size distribution for different depositional environments. *Groundwater* 52, 399–413.
- SCOTTISH ASSOCIATION FOR MARINE SCIENCE. 2013. SAMS Webcams & Weather [Online]. http://dalriada.sams.ac.uk/sams_weather/ [Accessed 27/11/2013].
- Stahl, H., Glud, A., Schroder, C.R., Klimant, I., Tengberg, A., Glud, R.N., 2006. Time-resolved pH imaging in marine sediments with a luminescent planar optode. *Limnol. Oceanogr. Methods* 4, 336–345.
- Stahl, H., Warnken, K.W., Sochaczewski, L., Glud, R.N., Davison, W., Zhang, H., 2012. A combined sensor for simultaneous high resolution 2-D imaging of oxygen and trace metals fluxes. *Limnol. Oceanogr. Methods* 10, 389–401.
- Stumm, W., Morgan, J.J., 1996. *Aquatic Chemistry: Chemical Equilibria and Rates in Natural Waters* Third Edition. John Wiley & Sons, Inc, New York, ISBN 0-471-51184-6.
- Tait, K., Stahl, H., Taylor, P., Widdicombe, S., 2015. Rapid response of the active microbial community to CO₂ exposure from a controlled sub-seabed CO₂ leak in Ardmucknish Bay (Oban, Scotland). *International Journal of Greenhouse Gas Control* 38, 171–181.
- Tankere-Muller, S., Zhang, H., Davison, W., Finke, N., Larsen, O., Stahl, H., Glud, R.N., 2007. Fine scale remobilisation of Fe, Mn, Co, Ni, Cu and Cd in contaminated marine sediment. *Mar. Chem.* 106, 192–207.
- Taylor, P., Stahl, H., Vardy, M., Bull, J., Ackhurst, M., Houghton, C., James, R., Lichtschlag, A., Long, D., Aleynik, D., Toberman, M., Naylor, M., Smith, D., Sayer, M., Widdicombe, S., Wright, I., Blackford, J., 2015. A novel sub-seabed CO₂ release experiment informing monitoring and impact assessment for geological carbon storage. *International Journal of Greenhouse Gas Control* 38, 13–17.
- The Global CCS Institute 2014, 2014. The Global Status of CCS: 2014. The Global CCS Institute, Canberra, Australia.
- Thorpe, S.A., Hall, A.J., 1983. The characteristics of breaking waves, bubble clouds, and near-surface currents observed using side-scan sonar. *Cont. Shelf Res.* 1, 353–384.

- Thorpe, S.A., Hall, A.J., Hunt, S., 1983. Bouncing internal bores of Ardmucknish Bay. Scotland Nat. 306, 167–169.
- Vizzini, S., Tomasello, A., Maida, G.D., Pirrotta, M., Mazzola, A., Calvo, S., 2010. Effect of explosive shallow hydrothermal vents on $\delta^{13}\text{C}$ and growth performance in the seagrass *Posidonia oceanica*. J. Ecol. 98, 1284–1291.
- Wang, J., WEI, H., Lu, Y., Zhao, L., 2013. Diffusive boundary layer influenced by bottom boundary hydrodynamics in tidal flows. J. Geophys. Res. Oceans 118, 5994–6005.
- Widdicombe, S., Spicer, J.I., 2008. Predicting the impact of ocean acidification on benthic biodiversity: what can animal physiology tell us? J. Exp. Mar. Biol. Ecol. 366, 187–197.
- Winkler, L.W., 1888. The Determination of Dissolved Oxygen in Water.
- Zeebe, R.E., Wolf-Gladrow, D.A., 2001. CO_2 in Seawater: Equilibrium, Kinetics, Isotopes. Third Impression (With Corrections) 2005. Elsevier Ltd, 84 Theobalds Road, London (WC1X *8RR, UK ISBN 0 444 50946 1).